# Slit Mask Design for the Giant Magellan Telescope Multi-object Astronomical and Cosmological Spectrograph

Darius S. Williams[1], Jennifer L. Marshall[2], Luke M. Schmidt[2], Travis Prochaska[2], Darren L. DePoy[2]

[1]*Case Western Reserve University,* [2]*Texas A&M University Department of Physics and Astronomy*

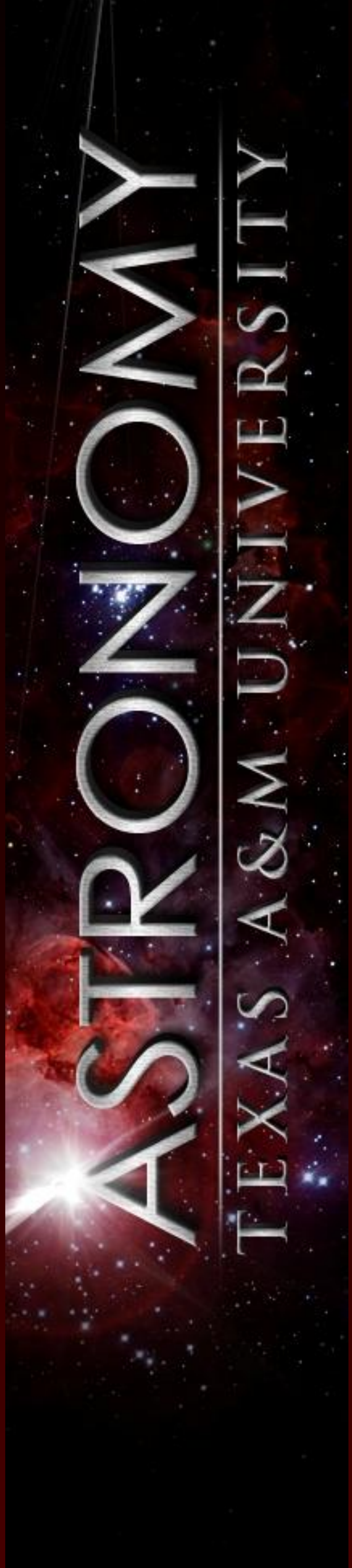


## Abstract

The Giant Magellan Telescope Multi-object Astronomical and Cosmological Spectrograph (GMACS) is currently in development for the Giant Magellan Telescope (GMT). GMACS will employ slit masks with a usable diameter of approximately 0.450m for the purpose of multi-slit spectroscopy. Of significant importance are the design constraints and parameters of the multi-object slit masks themselves as well as the means for mapping astronomical targets to physical mask locations. Analytical methods are utilized to quantify deformation effects on a potential slit mask due to thermal expansion and vignetting of target light cones. Finite element analysis (FEA) is utilized to simulate mask flexure in changing gravity vectors. The alpha version of the mask creation program for GMACS, GMACS Mask Simulator (GMS), a derivative of the OSMOS Mask Simulator (OMS), is introduced.

## Introduction

The GMACS slit mask will be a 500 mm x 500 mm spherical section (radius of curvature = 2.197 m) of metal sheet formed to match the best focal surface of the GMT Direct Gregorian Narrow-Field configuration. The area available for multi-slit spectroscopy is a circle centered on the mask with a diameter of approximately 450 mm and a focal scale of 1 arcsec mm$^{-1}$ (Schmidt, 2016). The slit mask's primary function, transmitting light for a selected catalog of targets, requires accuracy in accordance with the instrument's optical parameters and science goals.

Deformation in mask shape due to heating or gravity flexure potentially can lead to loss of targets or vignetting if slit edges shift to obscure all or part of a target. To prevent this, the mask material must be chosen such that working and manufacturing temperature fluctuations will not distort the mask beyond a slit width of 0.7 arcsec. Thickness of the mask, and thus the density of mask material used, must also be considered as to mitigate deviation from the best focal surface of the GMT. The nominal slit width was also used as a critical metric for comparing the gravitational distortion of the mask. The modeling and FEA program Solidworks was used to simulate the behavior of slit masks of various
compositions in varying gravity vectors.

OMS, a multi-object slit mask design program (Martini, 2012), was investigated as a potential foundation for the creation of an analogous program for GMACS due to physical similarities in mask design (Martini, 2011). OMS is a plug-in developed for ESO Skycat, a .fits and catalog viewer, which allows for the visualization, placement, and modification of slits on a projection of the instrument focal field and CCD footprint. The program outputs files in a machine-readable format suitable for manufacturing masks as well as a human-readable format for design verification and cross checking.

## Materials Tested

| Name | CTE [K$^{-1}$] | Density [kg m$^{-3}$] | Elasticity [N m$^{-2}$] | Poisson's Ratio |
|---|---|---|---|---|
| Aluminum 6061 | 2.4e-5 | 2700 | 6.9e+10 | 0.33 |
| Invar | 1.4e-6 | 8200 | 1.5e+11 | 0.30 |
| Nickel | 1.3e-5 | 8500 | 2.1e+11 | 0.31 |
| Aluminum Bronze | 1.7e-5 | 7400 | 1.1e+11 | 0.30 |
| Wrought Stainless Steel | 1.1e-5 | 8000 | 2.0e+11 | 0.26 |

Values are as reported in Davis (1998).

## Thermal Expansion

Mask distortion due to changes in temperature was explored both through linear analysis and an arc length method. Results of the linear analysis are presented in Fig. 1, and the arc length model and results for aluminum are presented in Fig. 2 and 3.

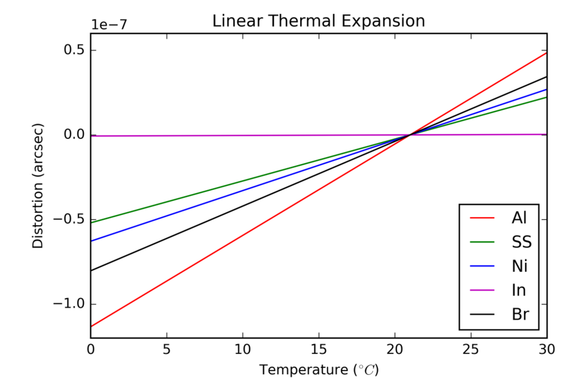


Figure 1.

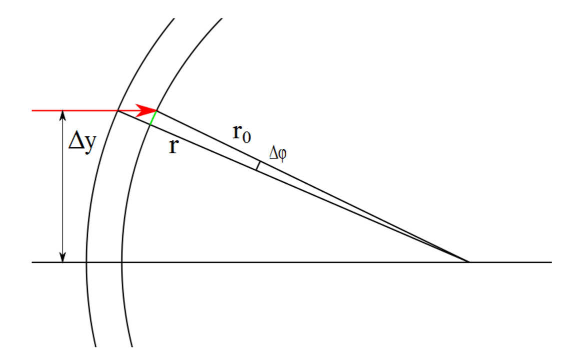

Figure 2. Here, $r_0$ is the radius of the slit mask that expands to a new radius r.

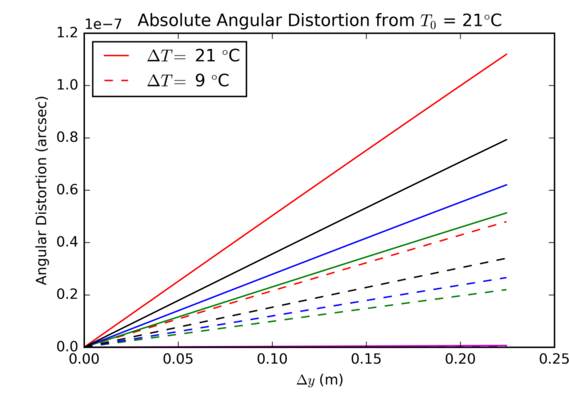


Figure 3. Colors are the same as in Fig. 1.

## Gravity Flexure

Using Solidworks, a model was created of the slit mask where parameters related to the material composition and thickness of the mask were used to see the magnitude and position of deformations. In these simulations, the mask was held fixed with rigid boundary conditions on all four sides and mask thickness was fixed at 1 mm. Fig. 4 shows the deformation regions of the mask in different gravity vectors. The maximum displacement values for the five mask materials considered in each of the three gravity vectors is plotted in Fig. 5.

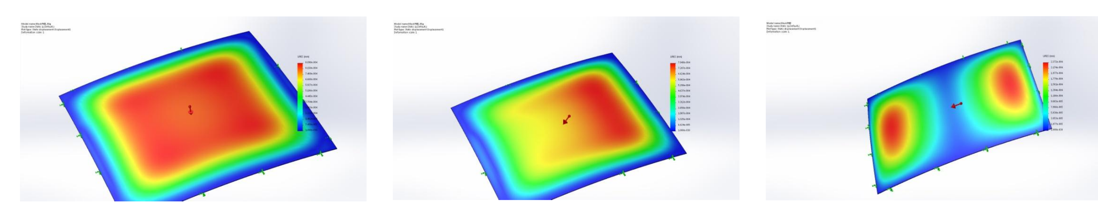

Figure 4. From left to right: horizontal (0°), 45°, and vertical (90°)

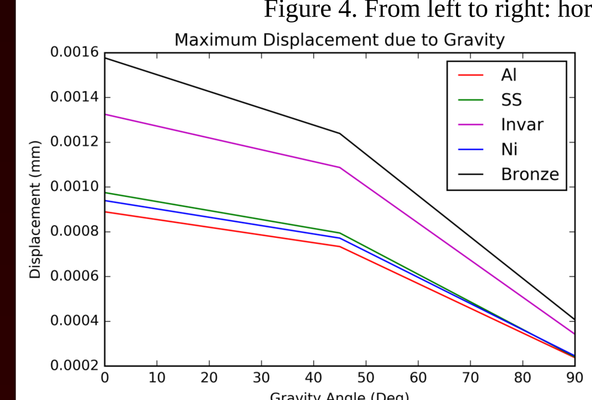


Figure 5.

Of the five materials simulated above, the three with the least amount of displacement, aluminum, stainless steel, and nickel, where chosen for a second simulation exploring the displacement as thickness was varied in a horizontal orientation. Boundary conditions are unchanged from the previous simulations. The results of this simulation are shown in Fig. 8 along with the reported mask thicknesses of a selection of spectrographs (dotted lines) (Becerril, 2010; Le Fèvre, 2003; Martini, 2011; Szeto, 1997). The Solidworks mesh size used was 0.004 m with a tolerance of 0.002 m.

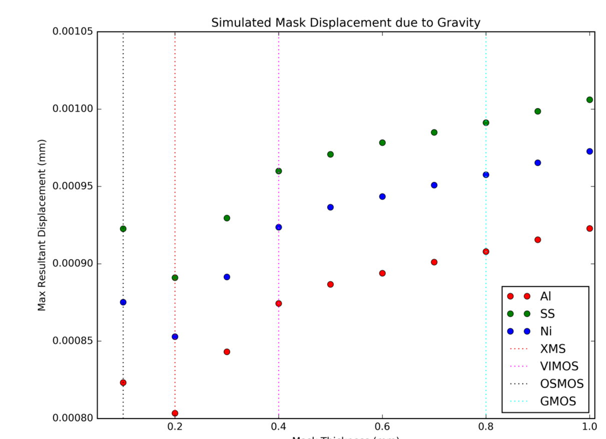


Figure 6.

## Vignetting

A geometric model was also created to determine the optimal angle for creating slits in the mask, i.e. the angle relative to the normal of the mask surface that extreme light rays would focus on the mask surface. A visualization of the model is shown in Fig. 7 and the results of the calculation are displayed in Fig. 8.

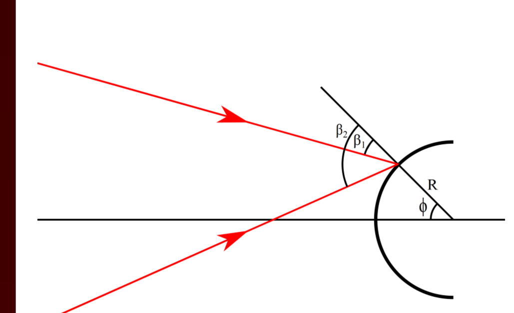

Figure 7. Here, R is the radius of the slit mask, and the upper and lower bounds of an incoming light cone are $\beta_1$ and $\beta_2$ respectively.

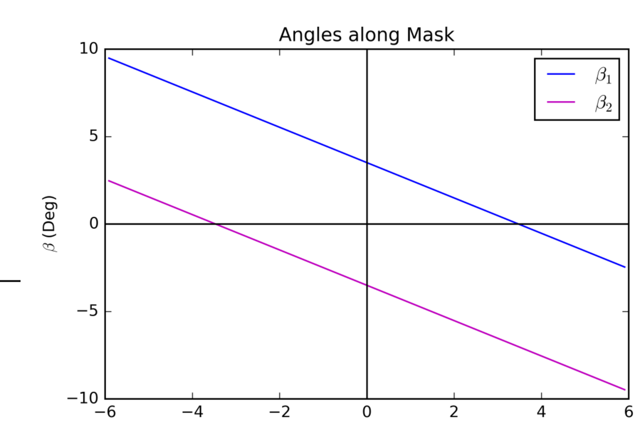


Figure 8.

## GMACS Mask Simulator

The code from OMS was modified to create a slit mask design and visualization software compatible with the instrument specifications of GMACS. GMS is a plug-in for ESO Skycat, a catalog and .fits viewer. Skycat is known to run on Linux and MacOS X. During development, GMS was tested using a virtual machine running Fedora 14. A screenshot displaying several of GMS's features is shown in Fig. 9.

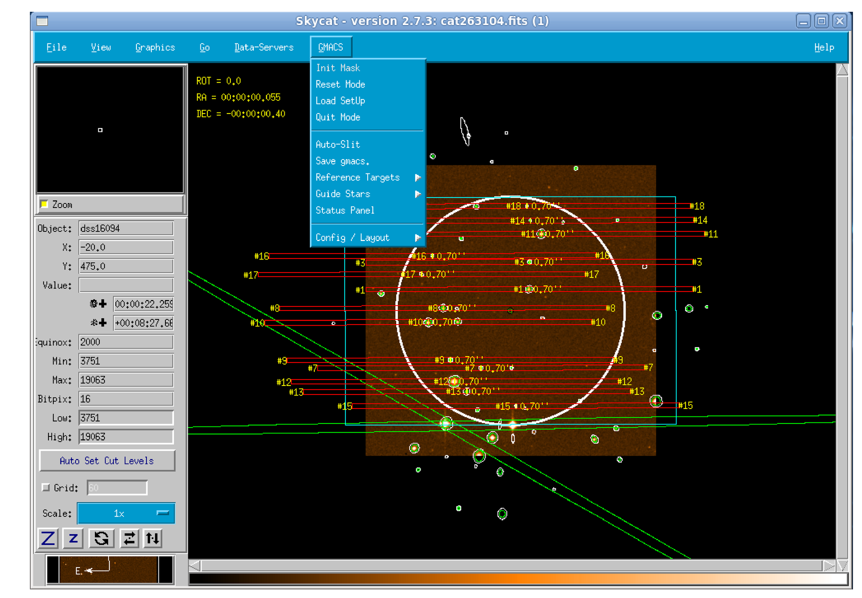

Figure 9. The cyan rectangle is the CCD footprint of the GMACS detector, and the white circle is the boundary of the instrument focal plane. After an image is loaded, a custom or online catalog can be initialized and create the various ellipses shown on the field which mark object locations. Using the 'Auto-Slit' function, shown in the drop-down menu above, creates the slits as shown above. When saved, the program outputs three files which can be used for manufacturing, visualization, and cross-checking of the mask template with expectations. As the underlying framework of GMS remains the same as OMS and the earlier LUCI Mask Simulator (LMS), a detailed overview of features can be found in the LMS User Manual (Hofman, 2010).

## Conclusions

The thermal expansion analyses all indicated a negligible (<< 0.7 arcsec) expansion of the mask relative to room temperature. Due to this, the mask material is unconstrained relative to the thermal expansion coefficient of the metal chosen.

In constraining mask thickness, the results from the Solidworks simulations provided the clearest indication of a thickness to minimize total mask deflection with a minimum that appears around 0.2 mm. However, the simulation results have not been rigorously tested for convergence. As such, the numerical values should not be taken as a final value. Further simulations that more finely sample the region around the minimum and properly test for convergence of the simulation with mesh settings would be necessary to more precisely define the optimal thickness by this method.

The results of simulations testing the mask flexure in different gravity vectors demonstrated that the mask geometry causes the most deformation in a horizontal orientation regardless of the material used for the specified boundary conditions. Further simulations or analyses would need to be done to see if this trend holds for more realistic boundary conditions that would correspond to an as-yet-decided method to rigidly hold a slit mask at the GMT focal plane.

In the simple geometric models used to estimate the vignetting of a target onto the mask surface, the optics of the GMT were not taken into consideration, and the results can at best be considered an upper limit of a hypothetical light cone's path. The results do, however, give an approximation to the angle a slit could need to be cut if a milling machine was used to create the slits.

The GMACS Mask Simulator is a preliminary step in the development of a mask design program for GMACS. As it is implemented currently, the software lacks features such as guide star selection and tracking as well as proper slit dispersion collision detection and slit length optimization, though these features among others could be implemented in future instances of GMS or a successor program. The biggest drawback of GMS in its current state is compatibility with more modern operating systems. Despite this, the program in its current state has the capacity to create slit mask templates which could be useful in testing manufacturing methods on future prototype slit masks.

## References

Becerril, S., Meisenheimer, K., Dubbeldam, C. M., Rohloff, R. R., Prada, F., Shanks, T., & Sharples, R. (2010). Extreme Multiplex Spectrograph: An efficient mechanical design for high-demanding requirements. arXiv preprint arXiv:1008.1227.

Davis, J. R. (1998). Metals handbook, desk edition (2nd ed.). ASM International.

Hofman, R. (2010). LUCIFER: LMS user manual. Retrieved from http://abell.as.arizona.edu/~lbtsci/Instruments/LUCIFER/Documents/LMS_UserManual_v160.pdf

Le Fèvre, O., Saïsse, M., Mancini, D., Brau-Nogué, S., Caputi, O., Castinel, L., ... & Mancini, G. (2003). Commissioning and performances of the VLT-VIMOS. In Proc. of SPIE Vol (Vol. 4841, p. 1671).

Martini, P., Stoll, R., Derwent, M. A., Zhelem, R., Atwood, B., Gonzalez, R., ... & Ward, B. (2011). The Ohio State Multi-Object Spectrograph. Publications of the Astronomical Society of the Pacific, 123(900), 187.

Martini, P. (2012). OMS user's manual. Retrieved from http://www.astronomy.ohio-state.edu/~martini/osmos/oms.html

Schmidt, L. M., Ribeiro, R., Taylor, K., Jones, D., Prochaska, T., DePoy, D. L., ... & Lee, H. I. (2016, August). Optical design concept for the Giant Magellan Telescope Multi-object Astronomical and Cosmological Spectrograph (GMACS). In Proc. of SPIE Vol (Vol. 9908, pp. 9908A4-1).

Szeto, K., Stilburn, J., Bond, T., Roberts, S., Sebesta, J., & Saddlemyer, L. (1997, March). Fabrication of Narrow-Slit Masks for the Gemini Multi-Object Spectrograph. In Proc. SPIE (Vol. 2871, pp. 1262-1271).

**Texas A&M University Department of Physics and Astronomy is an institutional member of:**

Munnerlyn Astronomical Instrumentation Lab, Texas A&M University

GMT

HETDEX – Hobby-Eberly Telescope Dark Energy Experiment – Illuminating the Darkness

LSST – Large Synoptic Survey Telescope

Dark Energy Survey

## Acknowledgments

Texas A&M University thanks Charles R. '62 and Judith G. Munnerlyn, George P. '40 and Cynthia Woods Mitchell, and their families for support of astronomical instrumentation activities in the Department of Physics and Astronomy.

This work was supported by NSF grant AST-1263034, "REU Site: Astronomical Research and Instrumentation at Texas A&M University."